

## References

- Angonin, M.C., Vanderriest, C., and Surdej J., 1990, in *Gravitational Lensing*, eds. Y. Mellier, B. Fort, G. Soucail (Springer-Verlag), 124.
- Kaysers, R., et al., 1990, *Ap. J.*, **364**, 15.
- Maaswinkel, F., et al., 1988a, *The Messenger*, **48**, 51.
- Maaswinkel, F., et al., 1988b, *The Messenger*, **51**, 41.
- Magain, P., et al., 1988, *Nature*, **334**, 325.
- Roddier, F., in *Progress in Optics*, XIX, ed. E. Wolf (North-Holland, Amsterdam), 281.

# A New Arc Candidate in a Compact Cluster

L. INFANTE, *Universidad Católica de Chile, Santiago, Chile*

E. GIRAUD, *ESO*

R. TRIAY, *Centre de Physique Théorique de Marseille, France*

## 1. Introduction

The number of arc candidates discovered in rich galaxy clusters over the past few years is less than about 10 (Fort, 1990). According to the lensing hypothesis, giant arcs such as those in Abell 370 and Cl 2244 are expected to be rarer than small arclets. Detecting faint arclets, however, requires doing photometry at extremely faint levels. While these objects can be used to trace the mass in clusters, they are not accessible to present-day spectroscopy. The number of reasonably good spectra of large arcs is still too small to prove that all distorted arc-like features are due to gravitational lensing. Hence it is crucial to substantially enlarge the sample of large arcs and obtain their redshifts.

The object presented here was discovered during a run of observations of rich clusters of galaxies. Our programme was not specifically designed to search for arc candidates. Nevertheless, since the observed clusters are rich and some are compact or have a compact core, they could have been included in a deep survey of arcs.

## 2. Results

The cluster (CL0017) was discovered on a deep CFHT prime focus plate in 1986 (Infante et al., 1986). It was first observed at La Silla during a non-photometric run of multispectroscopy with EFOSC at the 3.6-m ESO telescope. Measuring the redshift from red galaxies only, we find  $\langle z \rangle = 0.2716$ . A 600-s B exposure shows a possible arc-like feature centred on the extremely compact core of the cluster.

We reobserved the cluster with EMMI at the NTT obtaining short exposures in B, V, and R. Our purpose was to obtain quick relative photometry to select blue objects for a further run. The image presented in Figure 1 is from a 120-s R exposure (seeing 0.9"). It shows the ex-

tremely compact core of the cluster and a thin faint arc. Clusters with such a compact core are not frequent. We included it in our survey to check the velocity dispersion around the core and to study the galaxy population in this case. The centre of curvature of the arc lies in the cluster core, and the object is significantly bluer than the red cluster galaxies. The feature is seen (with more or less contrast) on all the images, suggesting that it is real. The image quality is poor, and deeper images are of

course necessary to study the object and confirm its appearance. The level of detection, however, is similar to that (for example) of the old (1975) video camera images of Abell 2218, Abell 379, and Cl2244 published by Petrosian, Bergmann and Lynds (1990) or those of Abell 963 obtained by Butcher et al. (1983). If confirmed, the arc will be accessible to spectroscopy using a purpose-made curved slit.

Using the red galaxies to probe the gravitational field around the cluster

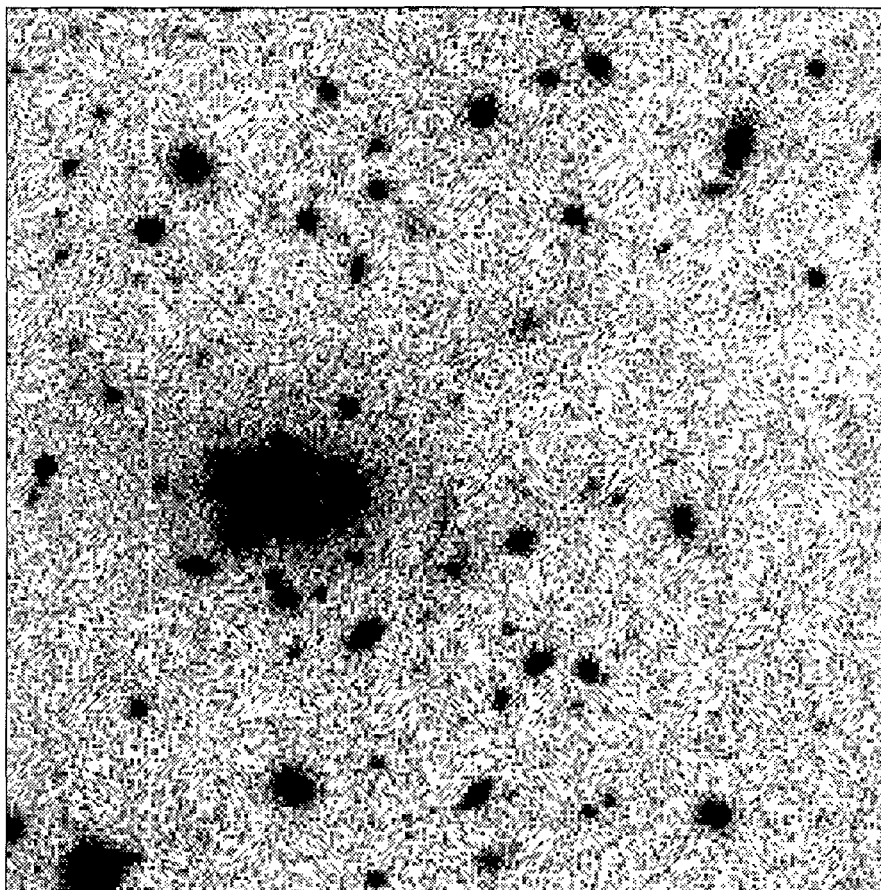


Figure 1: A section of a CCD frame in the R-band showing the very compact core of the cluster CL0017 and a thin faint arc-like feature (telescope: NTT; instrument: EMMI; exposure time: 2 min., seeing 0.9"). North is up and east is to the right.

core, we find a line-of-sight velocity dispersion of  $\sigma/(1+z) = 1300 \text{ km s}^{-1}$  for 19 objects, a very large value indeed. Thus finding an arc around such a massive and compact core would not be very surprising.

Pending the question of the reality of this feature, we believe that this class of cluster should receive high priority in a programme dedicated to the search for arcs. Will the object belong to the class of gravitational arcs? There are several classes of possible interlopers. The

most obvious are edge-on galaxies. Shells physically associated with certain cluster cores is a further possibility. Although the gravitational lens theory constrains the possible shapes of arc candidates, S-shaped features like the very well explained case in Cl 0500-24 (Giraud et al., 1989) show that the range of possibilities is not so small. Finally, a difference in colour between the arc and the red cluster galaxies is not by itself convincing since a blue object can lie almost at any redshift.

## References

Butcher H., Oemler, A., and Wells D.C., 1983, *Ap. J. Suppl.*, **52**, 183.  
 Fort B., 1990, in *Gravitational Lensing*, Eds. Y. Mellier, B. Fort, and G. Soucail (Springer-Verlag), p. 221.  
 Giraud E., Schneider P., and Wambsgans J., 1989, *The Messenger*, **56**, 62.  
 Infante L., Pritchett C.J., and Quintana H., 1986, *A.J.*, **91**, 217.  
 Petrosian V., Bergmann A.G., and Lynds R., 1990, in *Gravitational Lensing*, Eds. Y. Mellier, B. Fort, and G. Soucail (Springer-Verlag), p. 254.

# Broadband Imaging Performance of IRAC with the New Philips 64 × 64 Array

A. MONETI, A. MOORWOOD, G. FINGER, M. MEYER and H. GEMPERLEIN, ESO

## 1. Introduction

IRAC, ESO's general-user Infrared Array Camera, has recently been upgraded with a new 64 × 64 array from Philips Components. A general description of IRAC can be found in *The Messenger* (**52**, 50; and **54**, 56). The new array was installed in IRAC and tested on the ESO/MPI 2.2-m telescope during two test runs, the first one in January and the second in March 1991. The first test run was aimed primarily at studying the capabilities of the new array in the L band. In between the two runs, the performance of the array was improved somewhat by decreasing the read-out noise and improving charge transfer efficiency, and during the second run capabilities of the array for deep imaging were investigated in more detail. Overall, the new array is considerably better than the 32 × 32 array that had been in use since November 1989, but, as will be shown, it falls short of expectations on several grounds.

## 2. The Philips 64 × 64 Array

The basic characteristics of the new array are summarized in Table 1. Note the low read-out noise (RON) of the new array. The RON could be even lower:

with a presumed preamplifier gain of  $150e^-/ADU$  we were probably limited by the ADC resolution. Furthermore, in Section 6 we show that the actual gain may be as low as  $100 e^-/ADU$ , indicating a RON of  $\leq 65e^-$  RMS.

Since the pixel size has not changed, the same magnifications are available (0.3, 0.5, 0.8, and 1.6"/pix) as previously. Detector response is linear at least up to half-full wells when illuminated by a uniform background.

A typical bias frame has about 20 bad pixels, but the number of bad pixels increases with detector integration time (DIT), indicating that these pixels have high dark current. We will therefore call them "hot" pixels. There are about 120 hot pixels in a DIT = 30 sec dark frame.

From each hot pixel a long streak extends upwards and a short one extends to the right. These streaks are very prominent on dark exposures, and become progressively less prominent as the incident background increases. The streaks are probably due to trapping effects in the read-out CCD, and we are experimenting with the CCD electronics to try to reduce the problem.

The mean bias level is stable within  $\sim 20$  ADU. The precise level depends somewhat on the background level of

the previous frames, i.e. the array has some memory. This, however, is not a serious problem since (i) scientific observations are normally carried out in "beam switch" (b/s) mode, whereby a sky image is subtracted from the source image (the two images being acquired with the same integration time), and in the process the bias and the dark current are also subtracted; and (ii) flatfields have large enough signals that the uncertainty in the bias level is inconsequential.

## 3. Observations

During the first run, observations were carried out with both manual and automatic beam switching. In the latter mode, the telescope is moved automatically between the object position and a reference sky every 1–5 minutes. This mode was found to yield better quality data, and was subsequently used during the second run. Biases and flatfields were obtained throughout the runs, the latter were obtained on the day sky which provided a high signal in a short detector integration time (DIT), and hence flatfield frames with few hot pixels. The flatfields were then bias-subtracted and normalized to unity for use in data reduction.

Table 1: Array characteristics

Detector material	Hg:Cd:Te
Cutoff wavelength	$\sim 4.2 \mu\text{m}$
Read-out system	Buried channel CCD
Pixel size	$48 \mu\text{m}$
Read-out noise (RON)	$\leq 130e^-$ RMS
Dark current (at 49 K)	$\sim 300e^- \text{ sec}^{-1}$
Net detector quantum efficiency	$\sim 20\%$ at $2.2 \mu\text{m}$
Full well capacity	$9 \times 10^6 e^-$

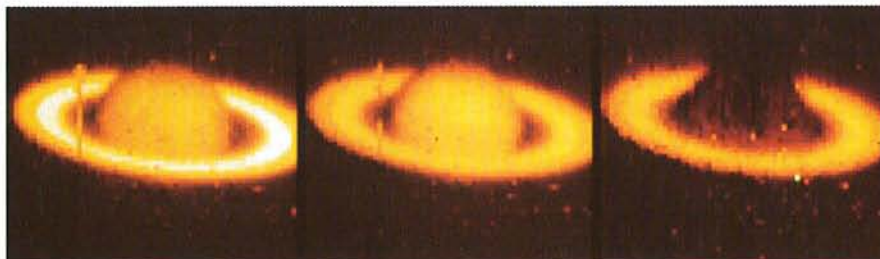


Figure 1: Saturn; from left to right: J, H, and K.